

Use of Stereotactic PET Images in Dosimetry Planning of Radiosurgery for Brain Tumors: Clinical Experience and Proposed Classification

Marc Levivier, MD, PhD¹; Nicolas Massager, MD¹; David Wikler, MS²; José Lorenzoni, MD¹; Salvador Ruiz, MD¹; Daniel Devriendt, MD³; Philippe David, MD⁴; Françoise Desmedt, MS³; Stéphane Simon, MS³; Paul Van Houtte, MD³; Jacques Brothchi, MD¹; and Serge Goldman, MD²

¹Department of Neurosurgery and Centre Gamma Knife, Hôpital Erasme and Université Libre de Bruxelles, Brussels, Belgium;

²PET/Biomedical Cyclotron Unit, Hôpital Erasme, Brussels, Belgium; ³Department of Radiation Therapy and Laboratory of Physics, Institut Jules Bordet, Brussels, Belgium; and ⁴Department of Radiology, Hôpital Erasme, Brussels, Belgium

We developed a technique that allows the routine integration of PET in stereotactic neurosurgery, including radiosurgery. We report our clinical experience with the combined use of metabolic (i.e., PET) and anatomic (i.e., MRI and CT) images for the radiosurgical treatment of brain tumors. We propose a classification describing the relative role of the information provided by PET in this multimodality image-guided approach. **Methods:** Between December 1999 and March 2003, 57 patients had stereotactic PET as part of their image acquisition for the planning of gamma knife radiosurgery. Together with stereotactic MRI and CT, stereotactic PET images were acquired on the same day using either ¹⁸F-FDG or ¹¹C-methionine. PET images were imported in the planning software for the radiosurgery dosimetry, and the target volume was defined using the combined information of PET and MRI or CT. To analyze the specific contribution of the PET findings, we propose a classification that reflects the strategy used to define the target volume.

Results: The patients were offered radiosurgery with PET guidance when their tumor was ill-defined and we anticipated some limitation of target definition on MRI alone. This represents 10% of the radiosurgery procedures performed in our center during the same period of time. There were 40 primary brain lesions, 7 metastases, and 10 pituitary adenomas. Abnormal PET uptake was found in 62 of 72 targets (86%), and this information altered significantly the MRI-defined tumor in 43 targets (69%). **Conclusion:** The integration of PET in radiosurgery provides additional information that opens new perspectives for the optimization of the treatment of brain tumors.

Key Words: PET; radiosurgery; gamma knife; stereotaxis; brain tumor

J Nucl Med 2004; 45:1146–1154

Radiosurgery is a stereotactic treatment defined as the delivery of a single, high dose of radiation allowing safe and complete destruction of precise target structures. It is proposed in the multimodality management of brain tumors. CT and MRI, the commonly used imaging modalities in radiosurgery, have limitations for target delineation in infiltrative tumors and postoperative conditions. We have proposed to integrate PET images in the dosimetry planning for Leksell Gamma Knife (LGK; Elekta A.B.) radiosurgery to improve targeting (1). The background of this approach is based on previous experience with PET in stereotactic conditions for brain biopsy (2). Briefly, it shows that PET data reflect extent, degree of anaplasia, and prognosis in brain tumors. Integration of PET in neurosurgical procedures may contribute to a better management of brain tumors, either in optimizing their delineation or in targeting the aggressive areas of heterogeneous tumors. This strategy has been initiated for the neurosurgical planning of brain tumor resection using neuronavigation (3). We here report on LGK radiosurgery guided by the combination of MRI or CT and PET stereotactic images. To evaluate the PET contribution, we propose a classification describing the relative role of PET and MRI in this multimodality image-guided approach.

MATERIALS AND METHODS

Patients and Preparation for LGK Radiosurgery

Between December 1999 and March 2003, 57 patients (32 males, 25 females; age, 3–77 y; mean age, 42 y) had stereotactic PET as part of imaging acquisition for LGK radiosurgery planning (Table 1). Standard preparation, as described (4), was similar for all patients undergoing LGK radiosurgery. Briefly, the Leksell G frame (Elekta A.B.) was attached to the patient's head under local anesthesia with mild sedation in adults or general anesthesia in children. Stereotactic CT was acquired as the quality control for MRI distortion. Stereotactic MRI was obtained using different images acquisition parameters. T1-weighted images before and after intravenous injection of gadolinium-diethylenetriaminepentaacetic acid (Gd-DTPA) were used in all patients as the primary

Received Sep. 25, 2003; revision accepted Jan. 29, 2004.

For correspondence or reprints contact: Marc Levivier, MD, PhD, Department of Neurosurgery and Gamma Knife Center, Université Libre de Bruxelles—Hôpital Erasme, 808 route de Lennik, B-1070 Brussels, Belgium.

E-mail: Marc.Levivier@ulb.ac.be

TABLE 1
Characteristics of Patients and LGK Treatment

Patient no.	Age (y)	Sex	Diagnosis	Previous brain surgery	Location, side	Radiotracer	Target volume (cm ³)	Prescription isodose volume (cm ³)	Dose/isodose (Gy/%)
1	36	M	Anaplastic astrocytoma	Open resection	Insula, R	¹⁸ F-FDG	7.10	10.80	15/55
2	34	M	Anaplastic astrocytoma	Stereotactic biopsy	Parietal, R	¹⁸ F-FDG	7.90	11.00	14/50
3	18	F	Pilocytic astrocytoma	Open resection	Brainstem	¹¹ C-Methionine	1.30	1.50	13/50
4	19	F	Pilocytic astrocytoma	Open resection	Hypothalamus	¹¹ C-Methionine	0.66	0.67	13/50
5	49	M	Glioblastoma	Open resection	Cerebellum	¹⁸ F-FDG	2.40	3.00	15/50
6	56	F	Low-grade glioma	Open resection	Temporal, R	¹⁸ F-FDG	1.70	2.90	15/50
7	52	F	Glioblastoma	Open resection	Parietal, R	¹⁸ F-FDG	2.73	5.10	15/50
8	39	M	Low-grade oligodendroglioma	Open resection	Parietal, L	¹⁸ F-FDG	6.40	8.00	15/50
9	59	M	Metastasis (lung)	Open resection	Frontal, R	¹⁸ F-FDG	6.80	8.00	18/45
10	23	M	Anaplastic ependymoma	Open resection	5 lesions	¹⁸ F-FDG	0.22–2.20	0.66–5.20	14–15/50–70
11	34	F	Anaplastic astrocytoma	Open resection	Cerebellar, R	¹¹ C-Methionine	7.30	7.80	14/50
12	3	F	Anaplastic ependymoma	Open resection	3 lesions	¹⁸ F-FDG	0.73–4.60	1.40–6.00	15/50
13	39	M	Anaplastic oligodendroglioma	Open resection, LGK	2 lesions	¹⁸ F-FDG	0.53–8.10	1.00–12.20	16/50
14	53	F	Neurocytoma	Stereotactic biopsy	3rd ventricle	¹¹ C-Methionine	1.40	1.60	15/50
15	53	M	Adenoma	Transphenoidal	Sella turcica	¹¹ C-Methionine	2.10	2.60	20/50
16	18	F	Adenoma	Transphenoidal	Sella turcica	¹¹ C-Methionine	0.40	0.49	35/50
17	39	M	Anaplastic oligodendroglioma	Open resection, LGK	2 lesions	¹⁸ F-FDG	0.85–1.20	1.20–1.50	16/50
18	56	F	Low-grade glioma	Stereotactic biopsy	Frontal, R	¹¹ C-Methionine	1.90	2.40	15/50
19	16	M	Atypical neurocytoma	Open resection	4 lesions	¹¹ C-Methionine	0.13–10.40	0.26–14.50	12–15/50
20	77	M	Metastasis (melanoma)	Open resection	Rolandic, L	¹⁸ F-FDG	8.80	11.80	18/50
21	43	M	Glioblastoma	Open resection	Prerolandic, R	¹⁸ F-FDG	3.60	5.70	16/50
22	67	F	Adenoma	Transphenoidal	Sella turcica	¹¹ C-Methionine	1.60	2.60	35/50
23	18	M	Pilocytic astrocytoma	Stereotactic biopsy	Cerebellar, L	¹¹ C-Methionine	0.55	0.78	15/45
24	36	F	Adenoma	Transphenoidal	Sella turcica	¹¹ C-Methionine	0.54	0.77	20/50
25	44	F	Low-grade oligodendroglioma	Stereotactic biopsy	Rolandic, R	¹¹ C-Methionine	4.10	4.90	12/50
26	53	F	Metastasis (pharynx)	None	2 lesions	¹⁸ F-FDG	0.58–9.20	0.82–13.80	18–20/40–50
27	58	F	Glioblastoma	Open resection	Frontal, L	¹⁸ F-FDG	3.90	9.80	15/50
28	23	F	Metastasis (melanoma)	Open resection	Cerebellar, L	¹⁸ F-FDG	0.98	1.20	20/50
29	39	F	Adenoma	Transphenoidal	Sella turcica	¹¹ C-Methionine	0.24	0.33	35/50
30	13	F	Low-grade glioma	Open resection	Brainstem	¹¹ C-Methionine	2.20	3.0	12/50
31	46	F	Metastasis (breast)	None	Meckel's cave	¹⁸ F-FDG	1.40	1.80	16/50
32	7	M	Pilocytic astrocytoma	Open resection	Temporal, R	¹¹ C-Methionine	1.0	1.80	15/50
33	18	F	Ganglioglioma	Open resection	Temporal, R	¹⁸ F-FDG	3.70	4.20	15/50
34	67	M	Glioblastoma	Open resection	Temporal, L	¹⁸ F-FDG	13.00	26.80	14/40
35	25	M	Adenoma	Transphenoidal	Sella turcica	¹¹ C-Methionine	1.80	3.00	20/50
36	14	F	Pilocytic astrocytoma	Open resection	Vermis	¹¹ C-Methionine	13.60	16.00	12/50
37	67	F	Glioblastoma	Open resection	Parietooccipital, R	¹⁸ F-FDG	2.60	6.00	18/50
38	44	F	Adenoma	Transphenoidal	Sella turcica	¹¹ C-Methionine	1.60	2.10	20/50
39	48	M	Glioblastoma	Open resection	Frontal, R	¹⁸ F-FDG	11.80	19.60	15/50
40	56	M	Pituitary adenoma	Transphenoidal	Sella turcica	¹¹ C-Methionine	6.00	7.70	20/50
41	48	M	Low-grade glioma	Open resection	Temporal, L	¹¹ C-Methionine	2.70	7.00	15/50
42	27	M	Ependymoma	Open resection	3rd ventricle, posterior	¹¹ C-Methionine	0.97–3.60	1.50–5.40	12–15/50
43	22	M	Low-grade oligodendroglioma	Stereotactic biopsy	Occipital, L	¹¹ C-Methionine	2.60	3.80	16/50
44	32	M	Glioblastoma	Open resection	Frontal, R	¹⁸ F-FDG	4.10	6.50	15/50
45	55	M	Glioblastoma	Open resection	Parietooccipital, R	¹⁸ F-FDG	3.60	10.40	15/50
46	58	M	Glioblastoma	Open resection	Temporoparietal, L	¹⁸ F-FDG	8.10	19.50	15/50
47	59	F	Pituitary adenoma	Transphenoidal	Sella turcica	¹¹ C-Methionine	0.41	0.58	30/50
48	44	F	Metastasis (breast)	LGK	Thalamic, R	¹¹ C-Methionine	6.70	8.20	18/50
49	49	M	Metastasis (lung carcinoma)	LGK	Multiple (2 lesions)	¹¹ C-Methionine	1.70–1.90	3.70–3.90	20/50
50	55	M	Glioblastoma	Open resection, LGK	Insula, R	¹⁸ F-FDG	1.80	4.70	18/50
51	31	M	Anaplastic astrocytoma	Open resection	Frontal, L	¹¹ C-Methionine	0.54	0.89	18/50
52	43	M	Glioblastoma	Open resection	Frontotemporal, L	¹⁸ F-FDG	11.60	25.40	15/50
53	72	M	Pituitary adenoma	Transphenoidal	Sella turcica	¹¹ C-Methionine	0.15	0.23	35/50
54	66	F	Glioblastoma	Open resection	Parietooccipital, L	¹¹ C-Methionine	11.80	20.40	15/50
55	33	M	Anaplastic astrocytoma	Stereotactic biopsy	Parietooccipital, L	¹¹ C-Methionine	0.67–3.04	3.20–6.30	15/50
56	56	M	Glioblastoma	Open resection	Rolandic, R	¹¹ C-Methionine	2.20	5.20	18/50
57	69	M	Glioblastoma	Open resection	Occipital, R	¹¹ C-Methionine	5.30	11.30	15/50

reference for target definition in this series. The patient was then transferred to the PET unit, which is adjacent to the MRI and Gamma Knife facilities.

Acquisition and Integration of Stereotactic PET Images

Acquisition of stereotactic PET images was originally described for brain biopsy (5,6). For LGK radiosurgery, stereotactic PET images were acquired with a Siemens/CTI ECAT 962 (HR+) tomograph, allowing the simultaneous acquisition of 63 planes with a slice thickness of 2.4 mm. PET image acquisition with the Leksell G frame was validated using a 3-dimensional (3D) acrylic phantom containing spheric simulated targets that can be imaged in both PET and CT and provides submillimeter spatial accuracy (1).

During PET data acquisition, the stereotactic frame is secured in the Elekta CT bed adapter together with a customized head holder fitted into the PET couch (Fig. 1). This allows fast and comparable positioning during CT, MRI, and PET. The radioactive fiducial markers are generated by a disposable tubing system embedded in a dedicated PET indicator box and filled with a ^{18}F -fluoride solution (0.37–0.74 MBq/mL) for the emission scan (Fig. 1). The patient is injected intravenously with either 222–333 MBq ^{18}F -FDG or 370–555 MBq ^{11}C -methionine, and 20-min images are acquired at 40 min for ^{18}F -FDG and at 20 min for ^{11}C -methionine.



FIGURE 1. Acrylic dedicated PET indicator box is attached to base ring of stereotactic Leksell G frame, which is secured in customized head holder during PET acquisition.

PET image files in CTI ECAT 7 format are transferred to the workstation used for the treatment planning with Leksell GammaPlan (LGP; Elekta A.B.) and converted in the LGP file format by custom software. The LGP PET software module results from an ongoing collaboration with Elekta R&D in the framework of a protocol approved by the Ethics Committee of our institution.

PET and MR Image Analysis and Definition of Target Volume

Planning begins with a separate analysis of each stereotactic imaging modality. A 3D volumetric contour is drawn on stereotactic MR images, most often corresponding to the area of Gd-DTPA enhancement. Then, the stereotactic PET images are analyzed independently, by the nuclear medicine physician and neurosurgeon together. Abnormal PET signal suitable for target definition corresponds either to areas of increased tracer uptake compared with the surrounding brain or to foci of relative increased tracer uptake in a hypometabolic lesion. A 3D volumetric PET contour delineating these areas is drawn on a visual basis or using the software-based segmentation algorithm and is projected onto the corresponding MR images. The final target volume is defined and drawn on the stereotactic MR image, taking into account the respective contributions of PET and MRI, as well as the anatomic location of the tumor and the functional areas at risk.

Dosimetry Planning and LGK Treatment

Once the target volume is defined, a dose plan is composed and verified by the neurosurgeon, radiation oncologist, and medical physicist. Multiple-isocenters planning is constructed to achieve the most conformal irradiation volume for the tumor. The prescribed dose is chosen on the basis of the nature of the tumor and the volume enclosed in the prescription isodose volume (Table 1). The radiosurgical treatment is performed with LGK C with Automatic Positioning System (APS) (7). After completion of the treatment, the stereotactic frame is removed; the patient is discharged from the hospital the next day.

Proposed Classification

To analyze the specific contribution of PET and MRI, in the definition of the target volume, we propose a 2-step classification that reflects the strategy used (Fig. 2). First, the relative location of the projection of PET and MRI volumes is considered, yielding 6 classes (class I, PET-defined volume projects within MRI-defined volume; class II, PET- and MRI-defined volumes do not fully project in the same areas; class III, MRI-defined volume projects within PET-defined volume; class IV, PET- and MRI-defined volumes are similar; class V, a PET volume can be defined and MRI is not contributive; class VI, a MRI volume can be defined and PET is not contributive). Based on these categories, a choice is made secondarily to define the target volume, categorizing subgroups A, B, and C, respectively, when only PET-, only MRI-, and a combination of the PET- and MRI-defined volumes are used to define the target volume (Fig. 2).

On this basis, contribution of PET is considered valuable in classes IA, IB, IIA, IIB, IIIA, IIIB, and V (Table 2). PET use is actually of different types. First, PET could be used to focus on the metabolically active part of the tumor when the MRI-defined volume is too large or most probably includes scar tissue (classes IA, IB, and IIA). Second, PET could be used to maximize a target volume underestimated on MRI (classes IIB, IIIA, and IIIB). Finally, PET could be used as the sole source of information for

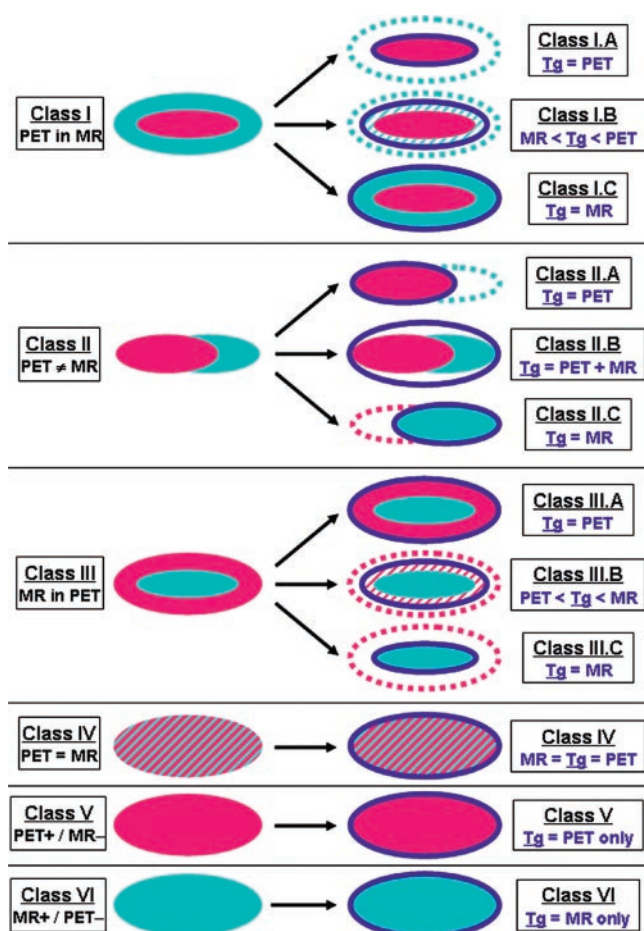


FIGURE 2. Proposed classification. Left column represents description of relative location of tumor volumes, as defined on basis of PET (purple) and MRI (light blue). Right column illustrates choice made to define final target volume (dark blue line). In classes I, II, and III, subclasses A, B, and C are defined (only PET-, only MRI-, and PET- and MRI-target volume definition).

targeting, when MRI is not informative (class V). PET findings are considered not useful in classes IC, IIC, IIIC, and IV, although an abnormal tracer uptake is detected. Finally, in class VI, PET cannot be used (no abnormal tracer uptake).

RESULTS

In all patients, stereotactic PET images were successfully acquired and integrated in the dosimetry planning within a 90-min period.

For all 57 treatment sessions, the patients were offered LGK radiosurgery with PET guidance (LGK-PET) because their tumor was ill-defined on MRI. This represents 10% of all radiosurgery procedures performed during the same time period ($n = 566$). LGK-PET was used in the following indications (Fig. 3A): 40 primary central nervous system (CNS) lesions (Fig. 4), 10 pituitary adenomas (Fig. 5), and 7 metastases (Fig. 6). ^{18}F -FDG was chosen in 26 patients (46%), and ^{11}C -methionine was chosen in 31 patients (54%) (Table 1; Fig. 3B). Radiotracer was chosen a priori, taking into account tumor histology, previous knowledge of its

TABLE 2
Usefulness of PET Information According to Proposed Classification

PET useful	PET not useful
Class IA Class IB	Class IC
Class IIA Class IIB	Class IIC
Class IIIA Class IIIB	Class IIIC Class IV
Class V	

Note that class VI is not included because there is no abnormal uptake on PET in this category.

metabolism, as well as the radiosurgical strategy envisioned. In high-grade tumors (including 1 atypical neurocytoma), ^{18}F -FDG was predominantly used (23/32 cases; 72%), aiming at a focal treatment on the most aggressive part of the tumor. In low-grade tumors, ^{11}C -methionine was predominantly used (22/25 cases; 88%), aiming at defining a maximized target. In 3 low-grade lesions, ^{18}F -FDG was used because an abnormal uptake of this radiotracer had

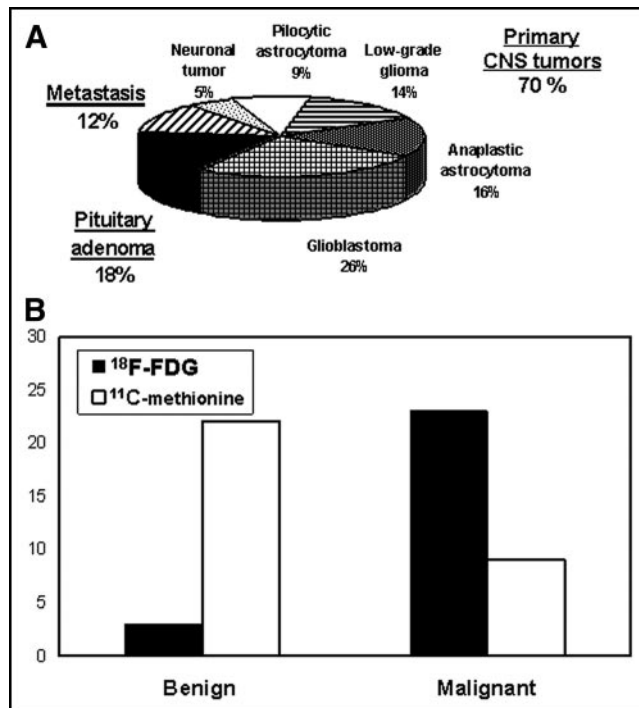
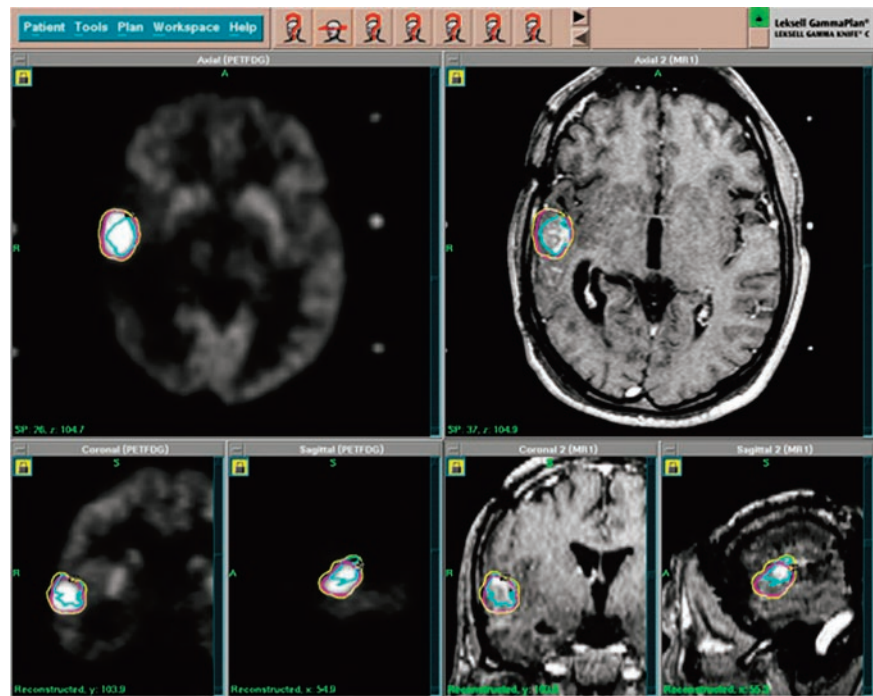


FIGURE 3. (A) Distribution of clinical indications for which PET was used for dosimetry planning of radiosurgery. (B) Distribution of relative use of ^{18}F -FDG and ^{11}C -methionine for data acquisition in low-grade and high-grade brain tumors.

FIGURE 4. Example of LGK radiosurgical planning using combined PET (with ^{18}F -FDG) and MRI in patient with recurrent anaplastic oligoastrocytoma, after surgeries, radiation therapy, and chemotherapy. Tumor volume is defined separately on PET (purple line, left images) and MRI (light blue line, right images): the 2 volumes project partially in different areas (class II). Final target volume includes both PET and MRI volumes (class IIB). Yellow line represents prescription isodose and encompasses the target volume.

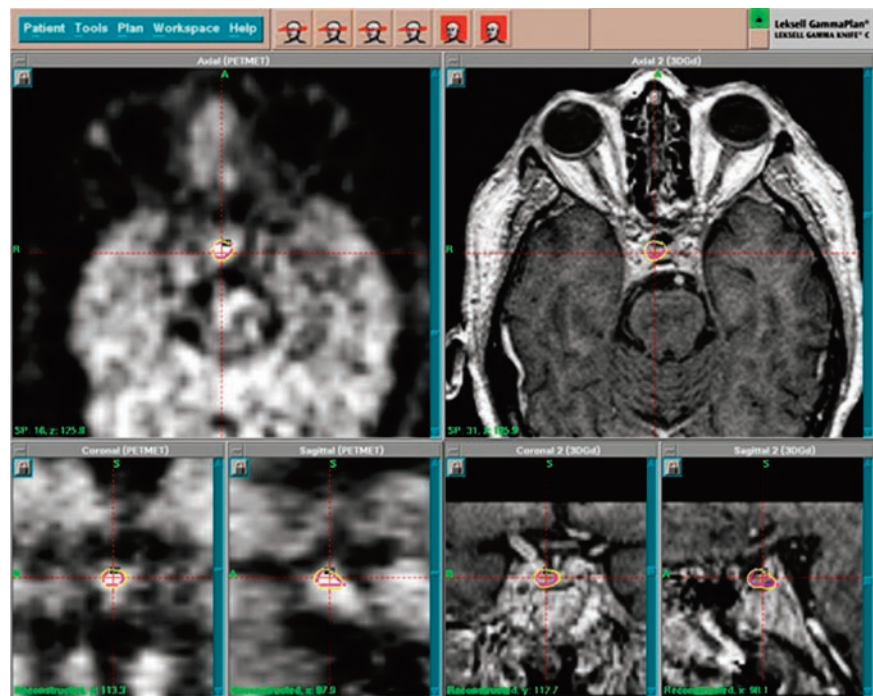


appeared during the follow-up, suggestive of malignant transformation.

Combining stereotactic PET and MRI information in LGP, 72 target volumes were defined for the 57 LGK-PET sessions, because 9 patients presented with multiple lesions or multifocal tumor areas. Seven of them had abnormal uptake of the tracer in all of their lesions (18 targets). One had no uptake in any of 5 lesions. One had no tracer uptake in 1 of 3 lesions of anaplastic ependymoma.

Altogether, there were 53 target volumes in primary CNS tumors (7 patients with multiple targets), 9 in metastases (1 patient with 2 metastases), and 10 in pituitary adenomas (no multiple targets). Table 3 summarizes the distribution of target volumes according to the proposed classification. The volume of PET uptake projected within the MRI-defined tumor (class I) in 26 targets (36.1% of all LGK-PET). In more than half of these cases (14 targets), the target volume was based primarily on PET information: Eleven target

FIGURE 5. Example of LGK radiosurgical planning using combined PET (with ^{11}C -methionine) and MRI in patient with recurrent adrenocorticotrophic hormone-secreting pituitary adenoma after transphenoidal surgery. Tumor volume cannot be clearly defined on MRI; therefore, only tumor volume defined on PET (purple line, left images) is used as final target volume (class V). Yellow line represents prescription isodose and encompasses target volume.



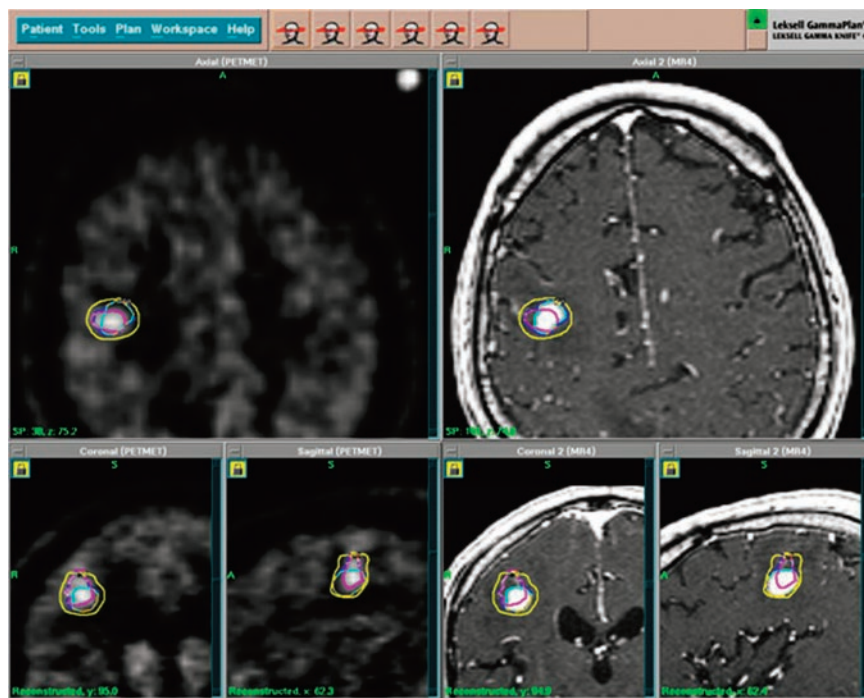


FIGURE 6. Example of LGK radiosurgical planning using combined PET (^{11}C -methionine) and MRI in patient with local recurrence of metastasis, previously treated with radiosurgery. Tumor volume is defined separately on PET (purple line, left images) and MRI (light blue line, right images); the 2 volumes project partially in different areas (class II). Final target volume (dark blue line) includes entirely both PET and MRI volumes (class IIB). Yellow line represents prescription isodose and encompasses target volume.

volumes were restricted to the area of PET uptake (class IA), and 3 target volumes comprised at least the entire area of PET uptake but not the entire abnormal MRI area (class IB), because the latter projected partially into highly functional areas. The 12 other target volumes were MRI-defined and included a smaller area of PET tracer uptake (class IC). Abnormal PET and MRI areas projected, at least partially, in different regions (class II) for 19 targets (26.4% of all LGK-PET). The target volume was based primarily on PET information in 16 cases, either because the target volume was restricted to the area of PET uptake (class IIA, 3 targets) or because the target volume included the entire PET and MRI abnormal areas (class IIB, 13 targets). In the

TABLE 3
Distribution of Target Volumes According
to Proposed Classification

Classification	No. of target volumes	% of total
Class I (PET in MRI)	26	36.1
IA	11	15.3
IB	3	4.2
IC	12	16.7
Class II (PET \neq MRI)	19	26.4
IIA	3	4.2
IIB	13	18.1
IIC	3	4.2
Class III (MRI in PET)	6	8.3
IIIA	5	6.9
IIIB	—	—
IIIC	1	1.4
Class IV (PET = MRI)	3	4.2
Class V (PET only)	8	11.1
Class VI (MRI only)	10	13.9

3 other cases, the target volume was based on MRI only (class IIC), because increased PET uptake was outside a safe MRI-defined volume. This corresponded to either ^{18}F -FDG uptake into displaced gray matter or tumor uptake extending in highly functional areas. The MRI-defined volume projected into a larger PET-defined volume (class III) in 6 targets (8.3% of all LGK-PET). The target volume included the entire PET volume (class IIIA) in 5 cases; in the others, the area of PET uptake that was outside of the MRI-defined volume projected into areas considered at risk for radiosurgery and was not included (class IIIC). PET was not used for target definition when PET- and MRI-defined volumes were similar (class IV) in 3 targets (4.2% of all LGK-PET). The area of increased PET uptake was used as the sole information to define the target volume (class V) in 8 targets (11.1% of all LGK-PET). Finally, there was no specific PET uptake (class VI) in 10 targets (13.9%). There was no situation of completely discordant PET and MRI results.

Altogether, abnormal PET uptake (all classes, except class VI) was found in 62 of the 72 lesions (86%). In these 62 lesions, the information obtained from stereotactic PET contributed to the definition of the target volume in 43 targets (69% of all positive PET; Fig. 7A). As shown in Figure 7B, in 25 targets (58% of useful PET; 40% of all positive PET), the target volume was based primarily on the area of increased PET uptake (classes IA, IB, IIA, and V). In those cases, stereotactic PET was used to focus the target volume on an area of high metabolism; the mean PET-defined volume was 3.1 cm^3 (range, $0.3\text{--}8.1 \text{ cm}^3$) and yielded to a mean target volume of 3.8 cm^3 (range, $0.5\text{--}8.1$

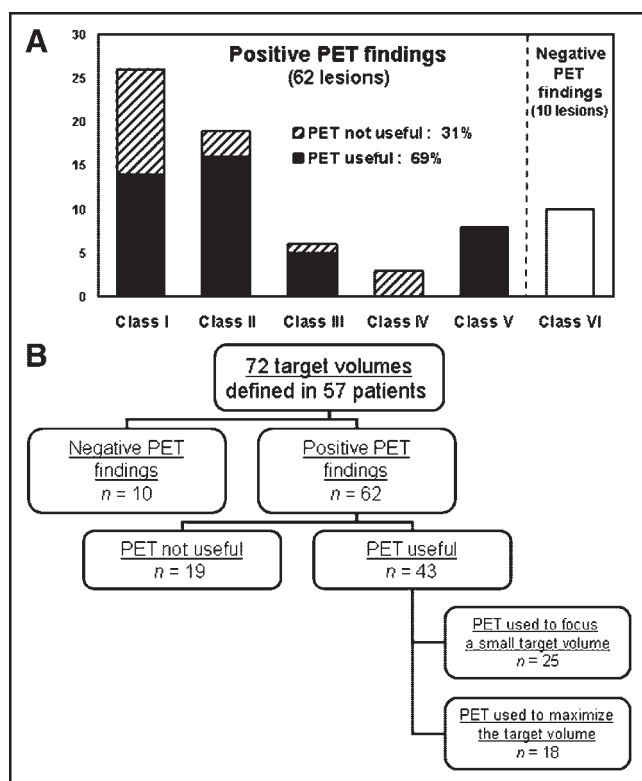


FIGURE 7. Distribution of 72 lesions according to proposed classification. (A) Contribution of PET findings for definition of final target volume is presented for each class. (B) Diagram illustrates how positive PET findings were used to define final target volume for radiosurgical treatment of brain tumors.

cm³) and a mean prescription isodose volume of 6.8 cm³ (range, 1.0–19.5 cm³). In the other 18 targets (42% of useful PET; 29% of all LGK-PET), the area of high PET uptake that projected partially outside of the MRI-defined tumor was included (classes IIB and IIIA). In those cases, stereotactic PET was used to identify tumor outside of the MRI-defined volume, yielding an increase of size of the target volume. The mean volume of the MRI-defined target was 5.2 cm³ (range, 0.1–10.8 cm³); the mean volume of the added PET-defined target was 1.5 cm³ (range, 0.05–10.9 cm³); this represents a mean increase of target volume of 132% (range, 2%–1,506%), yielding a mean target volume of 5.2 cm³ (range, 0.4–13.6 cm³) and a mean prescription isodose volume of 7.7 cm³ (range, 0.6–19.6 cm³). Finally, the PET uptake was not useful for target selection in 19 targets (31% of all positive PET); the mean target volume was 2.3 cm³ (range, 0.1–13.0 cm³) and the mean prescription isodose volume was 3.6 cm³ (range, 0.3–26.8 cm³).

We have noticed differences in the contribution of PET among the clinical indications. PET was considered useful in 34 of the 45 targets (76%) in primary CNS tumors, in 5 of the 8 targets (63%) in metastases, and in 4 of the 9 targets (44%) in pituitary adenomas. The numbers in each group are, however, currently insufficient to allow meaningful comparisons.

DISCUSSION

The goal of this article is to report on the feasibility of the routine integration of PET images in radiosurgery and to illustrate our clinical experience with this approach. There have been some early reports on the use of PET in radiosurgery, as an attempt of stereotactic localization (8), to evaluate the response to treatment (9,10) or to help in differentiating radiation necrosis from recurrence (11). PET had, however, not been fully incorporated yet into routine radiosurgical procedures, as described here. Both technically and clinically, this is a continuation of previous work on the integration of metabolic information in image-guided neurosurgery (3). The present analysis confirms that PET contains metabolic information that is independent of the morphologic information provided by CT or MRI. Therefore, PET integration in neurosurgical approaches, including radiosurgery, appears helpful for the management of brain tumors (2). Interestingly, similar approaches have been recently reported for the radiotherapy planning of gliomas with ¹²³I- α -methyltyrosine SPECT (12) and ¹⁸F-FDG PET (13).

PET Image Acquisition and Integration with Other Imaging Modalities

An imaging fiducial system is the most reliable way of PET registration to the patient's treatment space. Nevertheless, this requires careful solutions in addressing the various technical challenges associated with stereotactic PET acquisition, as discussed in details elsewhere (14). Phantom-based validation has been conducted to verify the application accuracy of the procedure (5). In our experience, fiducial registration mean error is about 0.2 mm for the volume, with a maximum value of about 0.6 mm for a higher error slice. Frameless stereotactic PET should extend accessibility to a larger number of radiosurgery centers. Comfort and flexibility would also benefit from this approach still under development.

Choice of Radiotracer for PET Images Used in Radiosurgery

Information obtained with PET mostly depends on the radiotracer used. ¹⁸F-FDG has proved helpful in assessing tumor persistence, progression, necrosis, or recurrence (15,16). Use of ¹⁸F-FDG has, nonetheless, some limitations. Most low-grade tumors have minor ¹⁸F-FDG uptake. Also, when a hypermetabolic lesion is in close relationship with the gray matter, tumor and normal ¹⁸F-FDG uptake are difficult to differentiate. Labeled amino acids represent an interesting alternative for the metabolic delineation of brain tumors (17,18). Indeed, PET with ¹¹C-methionine appeared helpful in tumors located in the gray matter and in low-grade gliomas.

In high-grade primary tumors of the CNS, PET with ¹⁸F-FDG was preferentially used to focus the treatment on a restricted volume corresponding to the most aggressive areas of the tumor. In metastases, PET with ¹⁸F-FDG differentiated tumor recurrence from scar tissue or necrosis,

helping in restricting the volume of treatment. In low-grade tumors and recurrent pituitary adenomas, PET with ^{11}C -methionine was mainly used to delineate their boundaries. The regional correlation between levels of ^{11}C -methionine and anaplastic changes (19) prompted us to consider the more sensitive ^{11}C -methionine for other purposes, such as restricted PET-based targeting within a larger area of tracer uptake. Further tests should be conducted with ^{18}F -labeled amino acids (17) to render this methodology accessible to centers without in-house tracer production.

Analysis of Stereotactic PET Images and Target Definition

Data acquisition and target selection with PET is as straightforward as with CT or MRI. In all stereotactic procedures (biopsy, open neurosurgery, and radiosurgery), we follow the same approach. The planning includes an independent analysis of the stereotactic PET for the delineation of a PET-defined volume, which projected onto the corresponding MRI volume. The final process of target definition on MRI is complex, primarily taking into account various aspects of the tumor, location of functional areas, and PET-defined volume. Actually, it integrates a larger set of information on clinical status, histology, and previous treatment. The whole procedure, therefore, implicates all physicians involved in imaging, surgical, and radiotherapeutic components. As a consequence, it is unrealistic, at this stage, to promote standardized definition of the target volume—for instance, using simple PET image thresholding—as proposed for lung cancer (20).

At the time of the planning, an assumption has to be made about the presence of tumor tissue in the entire area of increased PET tracer uptake. Indeed, image-based radiosurgical planning does not allow documentation of histology. Data correlating MRI findings with histology have been obtained with stereotactic biopsies of brain tumors (21). Along the same line, the relationship between pathology and metabolism found in stereotactic biopsy (19,22) and the increased knowledge about PET in brain tumor (23) strengthen the valuable link between PET uptake and histology in brain tumors. Moreover, the clinical context limits the risk of erroneous PET–MRI targeting since most targets are histologically defined inoperable or recurrent tumors. Of course, one cannot rule out that some PET-defined areas contain necrotic tissue, especially when treating recurrences after radiation therapy or previous radiosurgery. Recent papers addressing this issue support the use of PET in those conditions (13,24,25). Complementary investigations, such as with MR spectroscopy, may be helpful in that respect (26).

Indications of PET Integration in Radiosurgery

Integration of PET information in the dosimetry planning of radiosurgery has 2 goals: (a) to improve targeting in recognized indications for radiosurgery, such as metastases, and recurrent pituitary adenomas; and (b) to optimize tar-

geting for less-established indications, such as infiltrative primary tumors.

Radiosurgery is a well-established treatment of brain metastases, providing local tumor control and increased survival (27,28). However, local regrowth may occur, and the diagnosis between local recurrence and radiation-induced changes is difficult (29). In that respect, PET with ^{18}F -FDG has been considered to be helpful (11) and may serve as a basis for retreatment with LGK-PET. Still, in our experience, PET with ^{18}F -FDG seems to have a limited sensitivity in that indication. In the presence of negative ^{18}F -FDG PET, LGK-PET retreatment could be performed with ^{11}C -methionine in some patients.

Pituitary adenomas are best treated by surgical removal. Besides specific medical treatments, LGK radiosurgery is as an effective adjuvant therapy for recurrent or residual secreting and nonsecreting adenomas. However, the quality of the results mostly depends on the ability to define the target volume. Pituitary adenomas usually have a high uptake of ^{11}C -methionine, which may be in relation with their endocrine activity (30). We made similar observations and have started to prospectively include PET with ^{11}C -methionine in all radiosurgical planning for recurrent pituitary adenomas.

Radiosurgery may play a role as an adjuvant therapy for gliomas (31,32). However, because of their infiltrative nature, accurate delineation is difficult and the volume for treatment is limited. The use of well-defined metabolic data provided by PET may therefore be helpful for the radiosurgery of gliomas, as it is for brain biopsy targeting or tumor removal with neuronavigation (3). Indeed, PET improves the diagnostic yield of stereotactic brain biopsies (6), better delineates areas of anaplasia (19,22), better identifies tumor residues (15), and has a prognostic value independent of histology (33). On the same background, Tralins et al. (13) propose the use of PET with ^{18}F -FDG to define target volumes in the radiation dose escalation of glioblastomas.

Clinical Experience with Stereotactic PET in LGK Radiosurgery: Proposed Classification

Target volume definition is a crucial step in radiosurgery. The real clinical advantage of PET-based radiosurgical targeting needs comparative evaluations of local tumor control, functional results, and survival, ideally in matched randomized comparisons with current methods. The present study is a preliminary approach to this evaluation and, for that purpose, we developed a descriptive classification illustrating the relative information provided by PET and MRI. This classification identifies classes corresponding to different planning strategies with PET. In some instances, MRI disclosed a large abnormal volume that was not compatible with LGK radiosurgery, and PET was used to focus the treatment on active parts of the tumor. Conversely, in some cases, the target volume was maximized due to the use of PET when MRI underestimated tumor extent. Further accumulation of prospective data using this classification will allow us to better distinguish the type of contribution

PET provides in relation to the different clinical indications and the different radiopharmaceuticals available. The classification proposed will also allow us to accurately compare and categorize PET-based metabolic data and MRI-based anatomic data and, consequently, to better understand the metabolic changes that follow radiosurgery.

CONCLUSION

We have developed and used a technique allowing the routine integration of the metabolic images provided by PET in LGK radiosurgery. PET data are combined with MRI for defining the target volume of the radiosurgical treatment of patients with ill-defined or infiltrative brain tumors. A classification is proposed that is used to assess the benefit of PET information during the target volume definition and the radiosurgical planning. The integration of PET in LGK represents a crucial step toward further developments in radiosurgery, as this approach provides additional information that may open new perspectives for the optimization of the treatment of brain tumors.

ACKNOWLEDGMENTS

This work is financially supported by the Loterie Nationale, the Ministère de la Politique Scientifique, and the Fonds National de la Recherche Scientifique, Belgium. The Centre Gamma Knife of the Université Libre de Bruxelles is an official reference and training center of Elekta A.B., Sweden, for LGK C. The authors have no financial interests in the products of Elekta A.B. described in this article.

REFERENCES

- Levivier M, Wikler D, Goldman S, et al. Integration of the metabolic data of positron emission tomography in the dosimetry planning of radiosurgery with the gamma knife: early experience with brain tumors. *J Neurosurg.* 2000;93(suppl 3):233–238.
- Levivier M, Wikler D Jr, Massager N, et al. The integration of metabolic imaging in stereotactic procedures including radiosurgery: a review. *J Neurosurg.* 2002;97:542–550.
- Levivier M, Wikler D, Goldman S, Pirotte B, Brotschi J. Positron emission tomography in stereotactic conditions as a functional imaging technique for neurosurgical guidance. In: Alexander EB III, Maciunas RM, eds. *Advanced Neurosurgical Navigation*. New York, NY: Thieme Medical Publishers, Inc.; 1999:85–99.
- Lunsford LD, Flickinger JC, Coffey RJ. Stereotactic gamma knife radiosurgery: initial North American experience in 207 patients. *Arch Neurol.* 1990;47:169–175.
- Levivier M, Goldman S, Bidaut LM, et al. Positron emission tomography-guided stereotactic brain biopsy. *Neurosurgery.* 1992;31:792–797.
- Levivier M, Goldman S, Pirotte B, et al. Diagnostic yield of stereotactic brain biopsy guided by positron emission tomography with [¹⁸F]fluorodeoxyglucose. *J Neurosurg.* 1995;82:445–452.
- Levivier M, Ruiz S, Massager N, Lorenzoni J, Devriendt D, Brotschi J. The use of Leksell Gamma Knife C with automatic positioning system (APS) for the treatment of meningiomas and vestibular schwannomas. *Neurosurg Focus.* [serial online]. May 2003;14:Article 8:1–5.
- Zeck OF, Fang B, Mullani N, et al. PET and SPECT imaging for stereotactic localization. *Stereotact Funct Neurosurg.* 1995;64(suppl 1):147–154.
- Guo WY, Pan DHC, Liu S, et al. Early irradiation effects observed on magnetic resonance imaging and angiography, and positron emission tomography for arteriovenous malformations treated by gamma knife radiosurgery. *Stereotact Funct Neurosurg.* 1995;64(suppl 1):258–269.
- Ericson K, Kihlström L, Mogard J, et al. Positron emission tomography using [¹⁸F]fluorodeoxyglucose in patients with stereotactically irradiated brain metastases. *Stereotact Funct Neurosurg.* 1996;66(suppl 1):214–224.
- Mogard J, Kihlström L, Ericson K, Karlsson B, Guo W-Y, Stone-Elender S. Recurrent tumor vs radiation effects after Gamma Knife radiosurgery of intracerebral metastases: diagnosis with PET-FDG. *J Comput Assist Tomogr.* 1994;18:177–181.
- Grosu AL, Feldmann H, Dick S, et al. Implications of IMT-SPECT for postoperative radiotherapy planning in patients with gliomas. *Int J Radiat Oncol Biol Phys.* 2002;54:842–854.
- Tralins KS, Douglas JG, Stelzer KJ, et al. Volumetric analysis of [¹⁸F]-FDG PET in glioblastoma multiforme: prognostic information and possible role in definition of target volumes in radiation dose escalation. *J Nucl Med.* 2002;43:1667–1673.
- Levivier M, Wikler D, De Witte O, Massager N, Goldman S, Brotschi J. Positron emission tomography (PET) for the management of brain tumors. In: Black PM, Loeffler J, eds. *Cancer of the Nervous System*. 2nd ed. Philadelphia, PA: Lippincott Williams & Wilkins. In press.
- De Witte O, Levivier M, Violon P, Brotschi J, Goldman S. Quantitative imaging study of extent of surgical resection and prognosis of malignant astrocytomas. *Neurosurgery.* 1998;43:398–399.
- Levivier M, Becerra A, De Witte O, Brotschi J, Goldman S. Stereotactic biopsy for irradiated gliomas with disease progression. *J Neurosurg.* 1996;84:148–149.
- Wienhard K, Herholz K, Coenen HH, et al. Increased amino acid transport into brain tumors measured by PET of L-(2-¹⁸F)fluorotyrosine. *J Nucl Med.* 1991;32:1338–1346.
- Derlon JM, Petit-Taboué M-C, Chapon F, et al. The *in vivo* metabolic pattern of low-grade brain gliomas: a positron emission tomographic study using [¹⁸F]fluorodeoxyglucose and [¹¹C]-L-methylmethionine. *Neurosurgery.* 1997;40:276–288.
- Goldman S, Levivier M, Pirotte B, et al. Regional methionine and glucose metabolism in gliomas: a comparative study on PET-guided stereotactic biopsy. *J Nucl Med.* 1997;38:1–4.
- Erdi YE, Mawlawi O, Larson SM, et al. Segmentation of lung lesion volume by adaptive positron emission tomography image thresholding. *Cancer.* 1997;80:2505–2509.
- Kelly PJ, Daumas-Duport C, Scheithauer BW, Kall BA, Kispert DB. Stereotactic histologic correlations of computed tomography- and resonance imaging-defined abnormalities in patients with glial neoplasms. *Mayo Clin Proc.* 1987;62:450–459.
- Goldman S, Levivier M, Pirotte B, et al. Regional glucose metabolism and histopathology of gliomas: a study based on positron emission tomography-guided stereotactic biopsy. *Cancer.* 1996;78:1098–1106.
- Wong TZ, van der Westhuizen GJ, Coleman RE. Positron emission tomography imaging of brain tumors. *Neuroimaging Clin N Am.* 2002;12:615–626.
- Tsuyuguchi N, Sunada I, Iwai Y, et al. Methionine positron emission tomography of recurrent metastatic brain tumor and radiation necrosis after stereotactic radiosurgery: is a differential diagnosis possible? *J Neurosurg.* 2003;98:1056–1064.
- Belohlávek O, Simonova G, Kantorova I, Novotny J Jr, Liscák R. Brain metastases after stereotactic radiosurgery using the Leksell gamma knife: can FDG PET help to differentiate radionecrosis from tumour progression? *Eur J Nucl Med.* 2003;30:96–100.
- Rock JP, Hearshen D, Scarpace L, et al. Correlations between magnetic resonance spectroscopy and image-guided histopathology, with special attention to radiation necrosis. *Neurosurgery.* 2002;51:912–919.
- Sanghavi SN, Miranpuri SS, Chappell R, et al. Radiosurgery for patients with brain metastases: a multiinstitutional analysis, stratified by the RTOG recursive partitioning analysis method. *Int J Radiat Oncol Biol Phys.* 2001;51:426–434.
- Gerosa M, Nicolato A, Foroni R, et al. Gamma knife radiosurgery for brain metastases: a primary therapeutic option. *J Neurosurg.* 2002;97:515–524.
- Huber PE, Hawighorst H, Fuss M, Van Kaick G, Wannenmacher MF, Debus J. Transient enlargement of contrast uptake on MRI after linear accelerator (linac) stereotactic radiosurgery for brain metastases. *Int J Radiat Oncol Biol Phys.* 2001;49:1339–1349.
- Bergstrom M, Muhr C, Lundberg PO, Langstrom B. PET as a tool in the clinical evaluation of pituitary adenomas. *J Nucl Med.* 1991;32:610–615.
- Kondziolka D, Flickinger JC, Bissonette DJ, Bozik M, Lunsford LD. Survival benefit of stereotactic radiosurgery for patients with malignant glial neoplasms. *Neurosurgery.* 1997;41:776–785.
- Larson DA, Gutin PH, McDermott M, et al. Gamma knife for glioma: selection factors and survival. *Int J Radiat Oncol Biol Phys.* 1996;36:1045–1053.
- De Witte O, Levivier M, Violon P, et al. Prognostic value of positron emission tomography with [¹⁸F]fluoro-2-deoxy-D-glucose in the low-grade glioma. *Neurosurgery.* 1996;39:470–476.



The Journal of
NUCLEAR MEDICINE

Use of Stereotactic PET Images in Dosimetry Planning of Radiosurgery for Brain Tumors: Clinical Experience and Proposed Classification

Marc Levivier, Nicolas Massager, David Wikler, José Lorenzoni, Salvador Ruiz, Daniel Devriendt, Philippe David, Françoise Desmedt, Stéphane Simon, Paul Van Houtte, Jacques Brotchi and Serge Goldman

J Nucl Med. 2004;45:1146-1154.

This article and updated information are available at:
<http://jnm.snmjournals.org/content/45/7/1146>

Information about reproducing figures, tables, or other portions of this article can be found online at:
<http://jnm.snmjournals.org/site/misc/permission.xhtml>

Information about subscriptions to JNM can be found at:
<http://jnm.snmjournals.org/site/subscriptions/online.xhtml>

The Journal of Nuclear Medicine is published monthly.
SNMMI | Society of Nuclear Medicine and Molecular Imaging
1850 Samuel Morse Drive, Reston, VA 20190.
(Print ISSN: 0161-5505, Online ISSN: 2159-662X)

© Copyright 2004 SNMMI; all rights reserved.